*J. Anat.* (2005) **206**, pp535–542

# Beyond the initial axon segment of the spinal motor axon: fasciculated microtubules and polyribosomal clusters

Yan-Chao Li, Chang-Xie Cheng, Yong-Nan Li, Osamu Shimada and Saoko Atsumi

*Department of Anatomy, Interdisciplinary Graduate School of Medicine and Engineering, University of Yamanashi, Japan*

## Abstract

Dense undercoating, microtubular fascicles and scattered polyribosomal clusters have until now been considered to be the three structural features of the initial segment, and were thought not to extend beyond the initial segment into the myelinated parts of the axon. The aim of the present study was to make clear whether there is a sudden change in morphology between the unmyelinated and myelinated part. We followed spinal motor axons from the initial segment to the first internode by conventional electron microscopy and serial sectioning, and found that the microtubular fascicles and polyribosomal clusters do exist in the internodal axoplasm. The fasciculated microtubules were observed mainly in the first paranode. The polyribosomal clusters were found along the course of the first internode at a random distance, however, they occurred mainly in the proximal part of the first internode. The proportion of sections in which ribosomes were found, i.e. the incidence of ribosomes, in the first 30-μm-long portion was 71 ± 24% (mean ± SD, $n = 4$), and significantly different from that in the second 30-μm-long portion (3.2 ± 1.3%) (mean ± SD, $n = 4$) ($P < 0.005$). The more distal part of the first internode was not investigated.

**Key words** axons; chicken; electron microscopy; spinal motor neurons.

## Introduction

Spinal motor axons derive from the axon hillock or the proximal part of primary dendrites, beginning with an unmyelinated part called the initial segment. The initial segment is characterised by dense undercoating, fasciculated microtubules and scattered polyribosomal clusters (Palay et al. 1968; Peters et al. 1968; Conradi, 1969; Somogyi & Hamori, 1976; Sasaki et al. 1990). These features are the same for a variety of neuronal types and species (Peters et al. 1991). They are reported suddenly to stop at the initial segment endpoint, where myelination starts, and were not thought to exist in the internodes (Kohno, 1964; Palay et al. 1968; Peters et al. 1968, 1991). The first central internode of the motor axon is the first myelinated portion along the long course of such axons. Its proximity to the initial segment suggests that the first internode should be more similar to the initial segment in axoplasmic structure than more distal internodes. Conradi (1966) reported polyribosomes in the axoplasm of the myelinated portion near the first paranode of a cat spinal motor axon by transmission electron microscopy (TEM). However, because of the difficulty of accessibility and preservation there is little literature concerning the structure of the normal central internodes. The present study followed chicken spinal motor axons from the initial segment to the internodes by TEM of serial sections in order to determine whether there is a sudden morphological change between the unmyelinated and myelinated part. The chicken neuromuscular system has several advantages for muscle-nerve studies (Rafuse et al. 1996). For example, fast and slow primary myotubes are segregated into distinct fast and slow regions that are distributed in a characteristic spatial pattern (McLennan, 1983) so that the innervating motoneurons can be easily labelled by injecting horseradish peroxidase (HRP). This experiment belonged to a series of research on spinal fast and slow motoneurons, some findings of which have been recently published (Li et al. 2004).

Correspondence

*Dr Y.-C. Li, Department of Anatomy, Interdisciplinary Graduate School of Medicine and Engineering, University of Yamanashi 409–3898, 1110 Shimokato Tamaho-Cho, Yamanashi, Japan. T: +81-55-2741509; F: +81-55-2741509; E: ldlyc@yahoo.com, ldlyc3@yahoo.co.jp*

Accepted for publication *24 March 2005*

## Materials and methods

Sixteen 2- to 3-month-old chickens (*Gallus domesticus*), weighing 1–2 kg, were used for the experiment. This experiment was performed in accordance with the National Institute of Health Guide for the Care and Use of Laboratory Animals (NIH Publications no. 80–23) revised 1996 for the protection of animals, and was approved by the University of Yamanashi Animal Care and Use Committee.

In 14 chickens, motoneurons innervating the latissimus dorsi muscles in the spinal cord were retrogradely labeled by injecting HRP. After 18–24 h, each chicken was perfused through the heart with 1% paraformaldehyde and 1.25% glutaraldehyde in 0.1 M phosphate buffer (pH 7.4). The detailed procedures for HRP injection and perfusion fixation were described previously (Atsumi & Ohsato, 1984). In another experiment, two chickens, which were not injected with HRP into the muscle, were perfused with the same fixative. The cervical enlargements of the spinal cords were removed and sectioned at 50 μm in thickness with a Vibratome (Oxford Laboratories, St Louis, MO, USA). The HRP-labeled motoneurons were visualized after Diaminobenzidine (DAB) reaction and processed for TEM. The sections of the specimens without HRP treatment were stained in block in 70% ethanol containing 1% uranyl acetate for 2 h before dehydration and then embedded in Epon. Serial ultrathin sections were cut on an LKB 2088-V ultramicrotome (LKB-Produkter, Bramma, Sweden). The ultrathin sections were stained with uranyl acetate and lead citrate, examined with Hitachi H-7500 electron microscope (Hitachi, Tokyo, Japan). Electron micrographs were taken on film or obtained by CCD camera and stored in a computer. The dimensions of ribosomes and axons were measured with software MICROANALYZER ver.1.1b (Japanese Poladigital Co., Tokyo). The average thickness of ultrathin sections was estimated as 75 nm for a silver section or 120 nm for a gold section. The length of axon segments was measured by counting the number of all transverse ultrathin sections from the same segment and by multiplying the number by the section thickness.

A few transverse semithin (0.5–1 μm) sections were cut, stained with toluidine blue and examined with a light microscope. Guided by the semithin sections, the ultrathin sections were cut from the surface of the ventral grey matter to the neuronal soma. Most of motor axons were curved in the transverse as well as the sagittal plane, and thus the plane of section was adjusted so as to preserve the mode of transverse or longitudinal sectioning of the axons. In total, 19 axons, including three longitudinally and 16 transversely cut axons, were studied. Most were incomplete, and it was almost impossible to obtain an entire longitudinally cut first internode because of its long and curved course. Of the axons studied, four transversely cut axons (600–1400 sections per axon), which could be continuously followed from the initial segment endpoint to the first internode, were used for data analysis.

## Results

### General features of the initial segment and the first internode

The initial segments were 24–30 μm in length and tapered distally, ending immediately before myelination. There was no obvious difference between the axoplasmic structure of HRP-labeled motoneurons and unlabeled anterior horn large neurons, and these are described together. All figures represent specimens fixed in Os O4 (Osmium tetroxide), stained in block in uranyl acetate before dehydration and embedded in Epon.

The microtubules in the initial segment were arranged into characteristic fascicles (Fig. 1a). Within a fascicle, two or more microtubules were cross-linked by short filamentous strands with a centre-to-centre distance of 36–40 nm (Palay et al. 1968; Wuerker & Kirkpatrick, 1972; Nakazawa & Ishikawa, 1995). The dense undercoating under the axolemma stopped at the initial segment endpoint, the diameter of which was 46–68% of that of the internodal axons. In the distal part of the initial segment, mitochondria increased in number before the myelination (Figs 1a and 2) as previously reported (Li et al. 2004).

The dense undercoating became indistinguishable beneath the paranodal axolemma shortly after the initial segment ended (Fig. 1b,d).The following paranode was 1.6–4.0 μm in length, and thickened into the first internode (Fig. 2). The paranodal axoplasm contained fasciculated microtubules, which could be followed in the internode for 0.13–2.58 μm from the endpoint of the initial segment. Although fasciculated microtubules were found in almost all the four axons, they were difficult to distinguish in electron micrographs unless the axon profile was cut almost transversely. We counted the number of single and fasciculated microtubules at five different levels from the distal part of the initial segment to the first paranode of a well

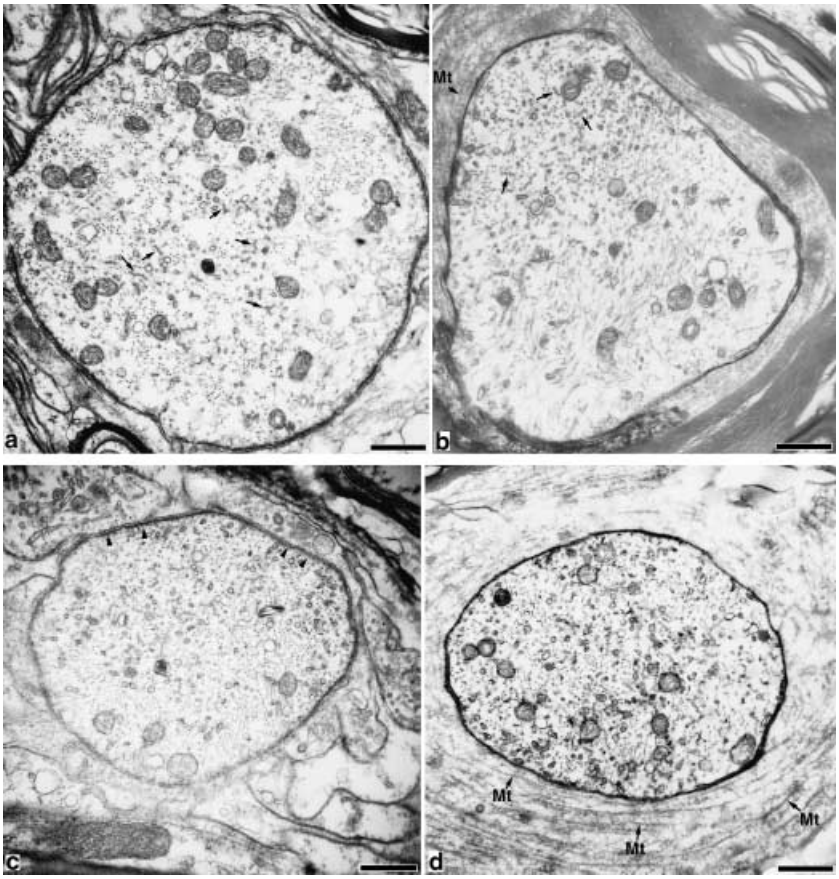


**Fig. 1** The initial segment and the first paranode of a spinal motor axon. Bar, 0.5 μm. (a) Distal part of the initial segment, where mitochondria accumulated. Microtubular fascicles are observed in the axoplasm (arrows). (b) Distal part of the first paranode. The paranodal axoplasm contains microtubular fascicles (arrows). (c) Endpoint of the initial segment. Beneath the axolemma, dense undercoating is observed (arrowheads). (d) Beginning of the first paranode. The periaxonal cytoplasm contained a great deal of spirally wound microtubules (arrows labelled with Mt).

**Table 1** Number of single microtubules and microtubular fascicles at five different levels from the distal part of the initial segment to the first paranode

| Level | Distance (μm) | Diameter (μm) | f1 | f2 | f3 | f4 | f5 | f6 | f7 | f8 | f9 | f10 | f11 | f12 | Total | Percentage number |
|---|---|---|---|---|---|---|---|---|---|---|---|---|---|---|---|---|
| IS | 1.32 | 2.30 | 24 | 25 | 18 | 8 | 6 | 1 | 1 | 1 | 1 | | | | 220 | 89 |
| ISend | 0.00 | 2.30 | 28 | 22 | 16 | 9 | 2 | 4 | 2 | | 1 | | | | 213 | 87 |
| Para1 | 0.30 | 2.47 | 18 | 23 | 15 | 7 | 6 | 2 | 1 | 1 | | 1 | | 1 | 216 | 92 |
| Para2 | 1.32 | 3.28 | 26 | 13 | 10 | 6 | 2 | 2 | | | | | | | 128 | 80 |
| Para3 | 1.40 | 3.32 | 26 | 9 | 6 | 5 | 1 | 1 | | | | | | | 93 | 72 |

f1, number of single microtubules; f2–f12, number of microtubular fascicles containing 2–12 microtubules. 'Total number', the total number of microtubules in a cross cut axon profile; 'percentage', the proportion of fasciculated microtubules in the total microtubules. The five levels are described in Fig. 2(a).

transversely cut axon (Table 1). Both the total number of microtubules and the percentage of fasciculated microtubules decreased in the myelinated part. The cytoplasm of myelin loops around the paranodal axon contained a great deal of spirally wound microtubules (Fig. 1b,d) (Spacek & Lieberman, 1980).

The diameter of the first internodal axon was more or less constant along its course, but the part following the paranode was moderately enlarged (Fig. 2). The length of the first internode examined was 62.1–103.7 μm (Table 2). Only one axon could be followed along the entire length of the first internode to the node of Ranvier, and the length of its first internode was 103.7 μm.

### Polyribosomal clusters in the first internode

Scattered clusters of polyribosomal particles are a well-known feature of the initial segment, but they were also present in the first internode. Ribosomes in all cell types of eukaryotic organisms have a similar size, and

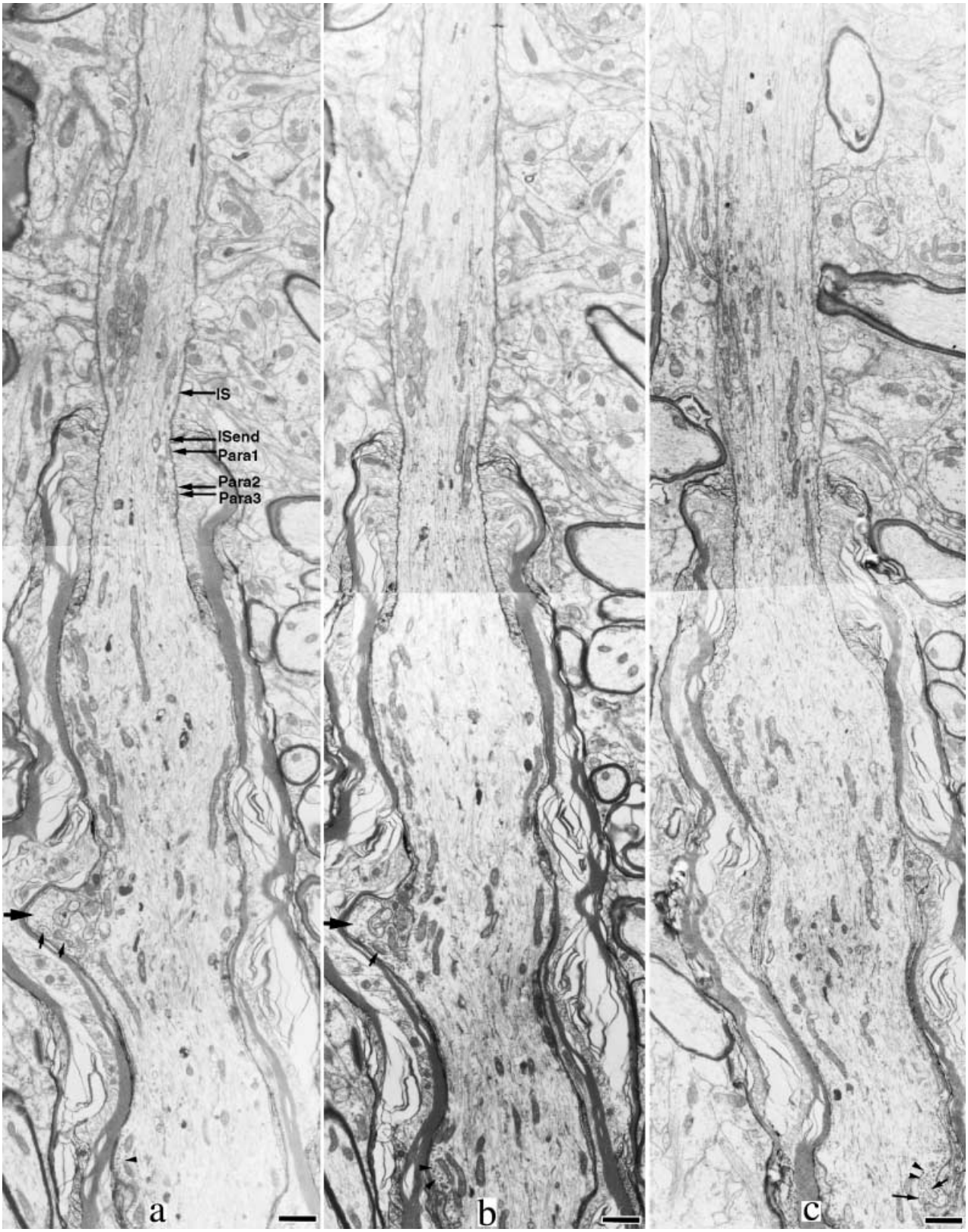


**Fig. 2** Serial electron micrographs of the distal part of the initial segment and the proximal part of the first internode. (a) Relative sites of five levels in Table 1 (IS, initial segment). Bar, 1.0 μm. The initial segment is the narrowest at the point where myelination starts. The paranode becomes thicker as the axon proceeds distally. The proximal part of the first internode shows a moderate enlargement. The internodal axon has a finger-like protrusion (large arrows). Near the axolemma, polyribosomes (arrowheads in panel c) and vesicular structures (small arrows) are observed.

**Table 2** The lengths of the first internode examined and the incidence of ribosomes in the internode

| Axon | Length of the first internode examined (μm) | The incidence (%) of ribosomes in | | |
|---|---|---|---|---|
| | | 0–30 (μm) | 30–60 (μm) | > 60 (μm) |
| A | 103.7 | 35 | 1.5% | 2.9% |
| B | 81.0 | 82 | 4.5% | 3.4% |
| C | 88.6 | 81 | 3.8% | 1.4% |
| D | 62.1 | 84 | 3.1% | |
| Mean ± SD | | 71 ± 24%* | 3.2 ± 1.3%* | |

The first internode of only axon A could be followed along the entire length. The number of sections containing ribosomes was counted in every 30-μm-long distance from the initial segment endpoint along the internode. The proportion (%) of sections in which ribosomes were found was defined by the incidence of ribosomes.
*Ribosomal incidences were significantly different between the first and second 30-μm-long portions ($P < 0.005$, student's *t*-test).

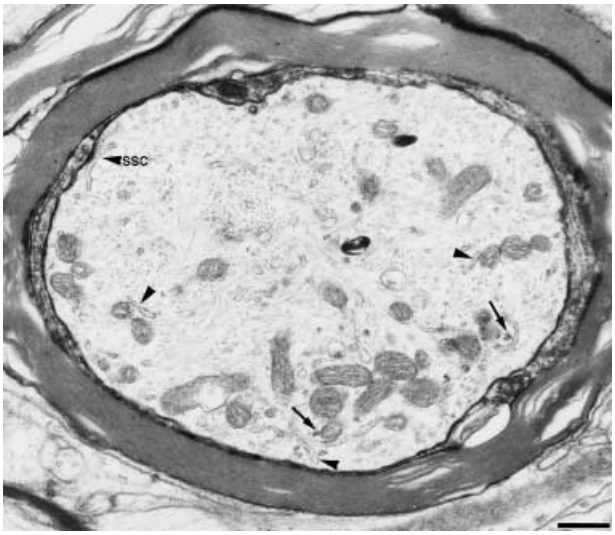


**Fig. 3** The proximal part of the first internode Polyribosomes (arrows) are localized in the peripheral axoplasm with mitochondria and smooth ER (arrowheads). Beneath the axolemma, a subsurface cistern is observed (arrowhead labelled with SSC). Bar, 0.5 μm.

the dimensions of ribosomes are constant (Zelena, 1972). In order to prove that the observed particles are in fact ribosomes, the diameter of the ribosome-like particles was measured and compared with that of ribosomes in adjacent oligodendrocytes. The values obtained were practically identical (22.2 ± 1.3 nm for axoplasmic ribosomes; 21.9 ± 1.1 nm for oligodendrocyte ribosomes). Similarly, the electron density of ribosomes in the axons was identical to that of the ribosomes in the adjacent oligodendrocytes.

Ribosomes were arranged in small clusters or rosettes suspending in the peripheral axoplasmic matrix (Figs 2–5). Many were localized in the vicinity of mitochondria, endoplasmic reticulum (ER) (Figs 3 and 4) or vesicular structures (Fig. 5b). These structural features distinguished them from glycogen granules or transversely cut cytoskeletal filaments. The distribution of polyribosomes in the axoplasm was different from that in dendrites (Fig. 5), and no rough ER was found in the axons. Electron-dense homogeneous structures of unknown nature were often found close to polyribosomes (Fig. 5b). Complex thin membrane-bounded structures were also often observed in the axoplasm. Their shapes varied and their membrane was similar to myelin sheath in electron density (Fig. 5b).The clusters of polyribosomes were found along the course of the first internode at various distances, but they occured mainly in the proximal part (about 30 μm) of the first internode.

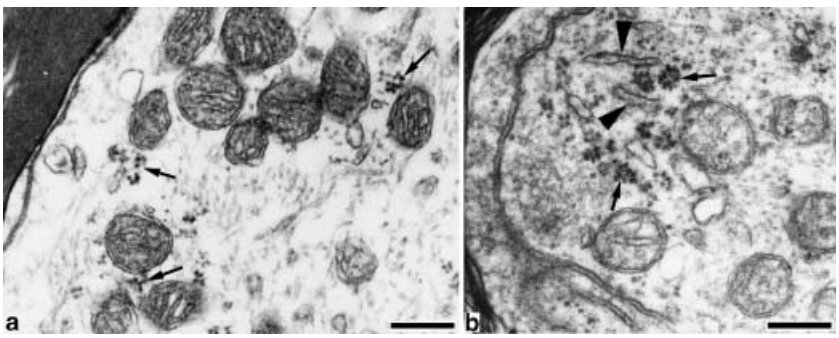


**Fig. 4** Polyribosomes in the first internode. Polyribosomes (arrows) are present in the axoplasmic periphery together with mitochondria and ER (arrowheads). Bar, 0.25 μm.

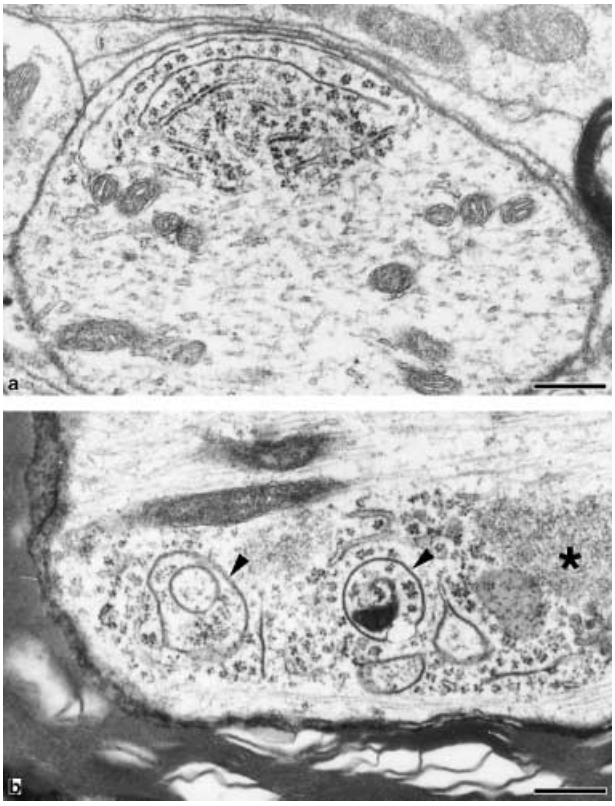


**Fig. 5** Polyribosomes in a dendrite (a) and in a myelinated axon (b). Polyribosomes are localized near the axolemma both in the dendrite and in the myelinated axon. No rough ER is found in the axon, however, thin membrane-bounded vesicular structures are observed among axoplasmic polyribosomes. The electron density of their membrane is similar to that of myelin sheath (arrowheads). A homogeneous electron-dense structure (*) is present. Bar, 0.25 μm.

Although they were occasionally observed in the more distal parts, they decreased in number and frequency. In order to quantify this impression, we counted the number of sections containing ribosomes every 30 μm from the initial segment endpoint along the internode. The proportion of sections in which ribosomes were found, i.e. the incidence of ribosomes, is shown in Table 2. This confirms a sharp decline in ribosomal incidence from 71% in the first 30-μm-long portion to 3.2% in the second 30-μm-long portion.

## Discussion

### General features of the initial segment and the first internode

The initial segment is well known as the initiation site of action potentials, and the dense undercoating is thought to be related to the initiation of action potentials. Consistent with the previous reports (Palay et al. 1968; Peters et al. 1968, 1991; Conradi, 1969; Somogyi & Hamori, 1976), the dense undercoating was not observed beyond the initial segment in the present study.

Fasciculated microtubules, another characteristic of the initial segment, were reported to occur in the axon hillock and to extend only as far as the beginning of the myelin sheath (Kohno, 1964; Palay et al. 1968; Peters et al. 1991). However, the present study shows that they also occur in the first paranode. Similarly, Nakazawa & Ishikawa (1995) reported microtubular fascicles in proximal nodes of Ranvier in rats, and found that the density of fasciculated microtubules tended to be higher in axon portions more proximal to the perikaryon. The limited incidence of these features suggests that they are not essential for the internode or nodal function. Nakazawa & Ishikawa (1995) suggest that this finding could be explained by microtubular cross-linking protein(s) being carried past the initial segment for some distance along the axon. However, if this were true, the cross-linking proteins must be prevented from having an action in the internode because few microtubular fascicles were found in the internodes.

### Polyribosomal clusters in the first internode

When ribosomes occur singly, they are difficult to distinguish by TEM from the transversely cut neurofilaments or heavy-metal-staining-induced structural ambiguities. In the first internode, polyribosomes are commonly arranged into characteristic clusters or rosettes and localized together with vesicles or ER in the periphery of axoplasm. Usually, mitochondria show a spatial proximity to ribosomes to supply energy for protein synthesis or to acquire nuclear-encoded mitochondrial proteins from polyribosomes (Giuditta et al. 2002). The characteristic rosettes of polyribosomes, their docking to ER and the occurrence in the vicinity of mitochondria (Zelena, 1972; Pannese & Ledda, 1991) make the polyribosomes stand out in the axoplasm. Additionally, the stability of their diameter and their similarity to those in the adjacent glial cells in size and electron density further distinguish the particles from glycogen granules and transversely cut neurofilaments. Polyribosomal clusters in myelinated motor axons were first described near the first paranode by Conradi (1966) in a study of the initial segment of cat spinal motor neurons; however, he paid little attention to this finding.

Thus far, there have been no similar reports on the first internode. Zelena (1972) detected polyribosomes in myelinated axons of rat dorsal root ganglia by TEM, and noted that the incidence of polyribosomes was highest within intraganglionic portions of rat axons, but was very low after the axon got outside the ganglia. The polyribosomes occurred on the myelinated side of the first node in almost each section, and were localized in randomly distributed restricted domain near the membrane along the axons, frequently in the vicinity of mitochondria. Consistent with this, Pannese & Ledda (1991) followed rabbit spinal nerves for a distance of 6.5–69.2 μm outside the ganglia and found few polyribosomes in most of them.

More precise methods, including electron spectroscopic imaging, RNA-sensitive YOYO-binding fluorescence and reactions of ribosome-specific antibodies, demonstrated the presence of ribosomes in the peripheral nervous system (PNS) portions of both unmyelinated and myelinated axons. These experiments showed that the ribosomal domains have a discrete, random intermittent distribution along the length of the axons, and are restricted to the peripheral zone of axoplasm (Giuditta, 1980; Giuditta et al. 1991; Koenig & Martin, 1996; Sotelo et al. 1999; Koenig et al. 2000; Bleher & Martin, 2001). A variety of evidence, mainly from experiments on squid giant axons, demonstrated that the axoplasmic RNAs are partially transferred from extra-axonal glia (Edstrom et al. 1969; Gainer et al. 1977; Lasek et al. 1977; Cutillo et al. 1983; Rapallino et al. 1988; Buchheit & Tytell, 1992). However, the glial–axonal transfer of proteins did not appear to involve the conventional secretory exocytic and endocytic pathways (Sheller et al. 1995).

As opposed to the squid giant axon, there are special structural complexities at the axonal–myelin sheath interface of vertebrate myelinated axons. In vertebrate CNS, the cytoplasm does not form a complete layer on the inside of the myelin of central sheaths, but instead is confined to a small part of the circumference on each side of the internal mesaxon (Peters et al. 1991). The small region of oligodendritic cytoplasm contains various organelles such as mitochondria, ER, vesicles and ribosomes, and intercellular macromolecular traffic transversing the periaxonal cleft that spans the internodal axon may occur (Alvarez et al. 2000). Conversely, the high incidence of ribosomes in very close proximity to the cell body suggests that they, like the microtubular cross-linking proteins, may simply be carried past the initial segment.

## Conclusion

The initial segment is defined morphologically as the portion of the initial part of the axon which extends from the axon hillock to the point immediately before the beginning of the myelin sheath. The structural features of the initial segment are the same for a variety of neuronal types and species, and had been thought not to continue beyond the initial segment. Consistent with the previous studies, the dense undercoating was not observed beyond the beginning of the myelin sheath in this study. However, both microtubular fascicles and polyribosomes were found in the following internode in the chicken spinal cord. Although microtubular fascicles did not extend beyond the paranode, the scattered clusters of polyribosomes occurred along the first internode with highest incidence in its proximal portion. This finding suggested that there are no sudden morphological change in the axoplasm between that of the initial segment and the first internode.

## References

**Alvarez J, Giuditta A, Koenig E** (2000) Protein synthesis in axons and terminals: significance for maintenance, plasticity and regulation of phenotype. With a critique of slow transport theory. *Prog. Neurobiol.* **62**, 1–62.

**Atsumi S, Ohsato K** (1984) Synaptology of alpha-motoneurons in the chicken spinal cord. *Neurosci. Res.* **2**, 77–96.

**Bleher R, Martin R** (2001) Ribosomes in the squid giant axon. *Neuroscience* **107**, 527–534.

**Buchheit TE, Tytell M** (1992) Transfer of molecules from glia to axon in the squid may be mediated by glial vesicles. *J. Neurobiol.* **23**, 217–230.

**Conradi S** (1966) Ultrastructural specialization of the initial axon segment of cat lumbar motoneurons. Preliminary observations. *Acta Soc. Med. Ups.* **71**, 281–284.

**Conradi S** (1969) Observations on the ultrastructure of the axon hillock and initial axon segment of lumbosacral motoneurons in the cat. *Acta Physiol. Scand. Supplement* **332**, 65–84.

**Cutillo V, Montagnese P, Gremo F, Casola L, Giuditta A** (1983) Origin of axoplasmic RNA in the squid giant fiber. *Neurochem. Res.* **8**, 1621–1634.

**Edstrom A, Edstrom JE, Hokfelt T** (1969) Sedimentation analysis of ribonucleic acid extracted from isolated Mauthner nerve fibre components. *J. Neurochem.* **16**, 53–66.

**Gainer H, Tasaki I, Lasek RJ** (1977) Evidence for the glia-neuron protein transfer hypothesis from intracellular profusion studies of squid giant axons. *J. Cell. Biol.* **74**, 524–530.

**Giuditta A** (1980) Origin of axoplasmic protein in the squid giant axon. *Riv. Biol.* **73**, 35–49.

**Giuditta A, Kaplan BB, van Minnen J, Alvarez J, Koenig E** (2002) Axonal and presynaptic protein synthesis: new insights into the biology of the neuron. *Trends Neurosci.* **25**, 400–404.

**Giuditta A, Menichini E, Perrone C, Langella M, Martin R, Castigli E, Kaplan BB** (1991) Active polysomes in the axoplasm of the squid giant axon. *J. Neurosci. Res.* **28**, 18–28.

**Koenig E, Martin R** (1996) Cortical plaque-like structures identify ribosome-containing domains in the Mauthner cell axon. *J. Neurosci.* **16**, 1400–1411.

**Koenig E, Martin R, Titmus M, Sotelo-Silveira JR** (2000) Cryptic peripheral ribosomal domains distributed intermittently along mammalian myelinated axons. *J. Neurosci.* **20**, 8390–8400.

**Kohno K** (1964) Neurotubules contained within the dendrite and axon of Purkinje cell of frog. *Bull. Tokyo Med. Dent. University* **11**, 411–442.

**Lasek RJ, Gainer H, Barker JL** (1977) Cell-to-cell transfer of glial proteins to the squid giant axon, The glia-neuron protein transfer hypothesis. *J. Cell Biol.* **74**, 501–523.

**Li YC, Zhai XY, Ohsato K, Futamata H, Shimada O, Atsumi S** (2004) Mitochondrial accumulation in the distal part of the initial segment of chicken spinal motoneurons. *Brain Res.* **1026**, 235–243.

**McLennan I** (1983) Differentiation of muscle fiber types in the chicken hindlimb. *Dev. Biol.* **97**, 222–228.

**Nakazawa E, Ishikawa H** (1995) Occurrence of fasciculated microtubules at nodes of Ranvier in rat spinal roots. *J. Neurocytol.* **24**, 399–407.

**Palay SL, Sotelo C, Peters A, Orkand PM** (1968) The axon hillock and the initial segment. *J. Cell Biol.* **38**, 193–201.

**Pannese E, Ledda M** (1991) Ribosomes in myelinated axons of the rabbit spinal ganglion neurons. *J. Submicrosc. Cytol. Pathol.* **23**, 33–38.

**Peters A, Palay SL, Webster H** (1991) The fine structure of the nervous system: *Neurons and Their Supporting Cells*, 3rd edn. Oxford, UK: Oxford University Press, pp. 101–234.

**Peters A, Proskauer CC, Kaiserman-Abramof IR** (1968) The small pyramidal neuron of the rat cerebral cortex. The axon hillock and initial segment. *J. Cell Biol.* **39**, 604–619.

**Rafuse VF, Milner LD, Landmesser LT** (1996) Selective innervation of fast and slow muscle regions during early chick neuromuscular development. *J. Neurosci.* **16**, 6864–6877.

**Rapallino MV, Cupello A, Giuditta A** (1988) Axoplasmic RNA species synthesized in the isolated squid giant axon. *Neurochem. Res.* **13**, 625–631.

**Sasaki S, Maruyama S, Takeishi M** (1990) Observation of the proximal portions of axons of anterior-horn cells in the human spinal cord. *Acta Anat (Basel)* **139**, 26–30.

**Sheller RA, Tytell M, Smyers M, Bittner GD** (1995) Glia-to-axon communication: enrichment of glial proteins transferred to the squid giant axon. *J. Neurosci. Res.* **41**, 324–334.

**Somogyi P, Hamori J** (1976) A quantitative electron microscopic study of the Purkinje cell axon initial segment. *Neuroscience* **1**, 361–365.

**Sotelo JR, Kun A, Benech JC, Giuditta A, Morillas J, Benech CR** (1999) Ribosomes and polyribosomes are present in the squid giant axon: an immunocytochemical study. *Neuroscience* **90**, 705–715.

**Spacek J, Lieberman AR** (1980) The presence and possible significance of agranular reticulum in paranodal oligodendrocyte cytoplasm and in periglomerular astrocyte processes. *Brain Res.* **196**, 498–501.

**Wuerker RB, Kirkpatrick JB** (1972) Neuronal microtubules, neurofilaments, and microfilaments. *Int. Rev. Cytol.* **33**, 45–75.

**Zelena J** (1972) Ribosomes in myelinated axons of dorsal root ganglia. *Z. Zellforsch Mikrosk Anat* **124**, 217–229.